Received: 4 September 2017 | Accepted: 6 November 2017

DOI: 10.1111/jpi.12455

ORIGINAL ARTICLE

WILEY Journal of Pineal Research
Molecular, Biological, Physiological and Clinical Aspects of Melatonin

# Melatonin alleviates adipose inflammation through elevating α-ketoglutarate and diverting adipose-derived exosomes to macrophages in mice

**Zhenjiang Liu** | **Lu Gan** | **Tiantian Zhang** | **Qian Ren** | **Chao Sun**

College of Animal Science and Technology, Northwest A&F University, Yangling, Shaanxi, China

**Correspondence**
Chao Sun, College of Animal Science and Technology, Northwest A&F University, Yangling, Shaanxi, China.
Email: sunchao2775@163.com

**Funding information**
Major National Scientific Research Projects, Grant/Award Number: 2015CB943102; National Nature Science Foundation of China, Grant/Award Number: 31572365; Key Sci-tech innovation team of Shaanxi province, Grant/Award Number: 2017KCT-24; Fundamental Research Funds for the Central Universities, Grant/Award Number: 2452017084

**Abstract**

Obesity is associated with macrophage infiltration and metabolic inflammation, both of which promote metabolic disease progression. Melatonin is reported to possess anti-inflammatory properties by inhibiting inflammatory response of adipocytes and macrophages activation. However, the effects of melatonin on the communication between adipocytes and macrophages during adipose inflammation remain elusive. Here, we demonstrated melatonin alleviated inflammation and elevated α-ketoglutarate (αKG) level in adipose tissue of obese mice. Mitochondrial *isocitrate dehydrogenase 2* (*Idh2*) mRNA level was also elevated by melatonin in adipocytes leading to increase αKG level. Further analysis revealed αKG was the target for melatonin inhibition of adipose inflammation. Moreover, sirtuin 1 (Sirt1) physically interacted with IDH2 and formed a complex to increase the circadian amplitude of *Idh2* and αKG content in melatonin-inhibited adipose inflammation. Notably, melatonin promoted exosomes secretion from adipocyte and increased adipose-derived exosomal αKG level. Our results also confirmed that melatonin alleviated adipocyte inflammation and increased ratio of M2 to M1 macrophages by transporting of exosomal αKG to macrophages and promoting TET-mediated DNA demethylation. Furthermore, exosomal αKG attenuated signal transducers and activators of transduction-3 (STAT3)/NF-κB signal by its receptor oxoglutarate receptor 1 (OXGR1) in adipocytes. Melatonin also attenuated adipose inflammation and deceased macrophage number in chronic jet-lag mice. In summary, our results demonstrate melatonin alleviates metabolic inflammation by increasing cellular and exosomal αKG level in adipose tissue. Our data reveal a novel function of melatonin on adipocytes and macrophages communication, suggesting a new potential therapy for melatonin to prevent and treat obesity caused systemic inflammatory disease.

**KEYWORDS**

α-ketoglutarate, adipose inflammation, exosome, macrophage, melatonin

## 1 | INTRODUCTION

Obesity is a complex chronic disease and becomes a public health epidemic worldwide.[1] Evidence suggests that inflammation is a central and reversible process in obesity and its comorbidities including type 2 diabetes, cardiovascular diseases, and neurodegenerative diseases.[2,3] Obesity-associated low-grade and chronic inflammation are characterized by infiltration and activation of immune cells in adipose tissue.[4] In particular, adipose tissue macrophages communicate with

adipocytes and thereby lead to obesity-associated alterations in the microenvironment of adipose tissue.[5,6] Recent evidences demonstrate that tricarboxylic acid (TCA) cycle and its endogenous metabolites are critical in orchestrating metabolic inflammation in obese adipose tissue.[7,8] Thus, these findings provide a potential new anti-inflammatory approach for the regulation of metabolic inflammation to prevent obesity-associated metabolic diseases.

Melatonin (N-acetyl-5-methoxytryptamine) is mainly synthesized by the pineal gland and maintains circadian rhythm in mammals.[9-11] Melatonin presents multiple physiological functions including antioxidant, anti-inflammatory, immunomodulatory, and oncostatic effects.[12-14] Many actions of melatonin are mediated through interaction with the melatonin receptors 1 and 2 (MT1 and MT2), which are G-protein-coupled membrane receptors found in several cell types, including immune cells.[15,16] Studies demonstrate melatonin ameliorates low-grade inflammation and oxidative stress by repressing the inflammatory response in brain and peripheral tissues.[17-19] Furthermore, melatonin could counteract the immune alterations and trigger an effective balance of innate and humoral immune response in immune cells.[20-22] Exogenous melatonin enhances antigen presentation by splenic macrophages to T cells in mice.[23,24] Recent studies suggest that melatonin suppresses lipopolysaccharide (LPS)-induced pro-inflammatory factors release in macrophages.[25] Our previous study has proposed that melatonin promotes proliferation and alleviates inflammasome-induced pyroptosis in adipocytes.[26,27] However, the effects of melatonin on the communication of adipocytes and macrophages during peripheral adipose inflammation remain elusive. Exosomes, the small vesicles, are increasingly recognized as important mediators of intercellular communication, being involved in the transmission of biological signals between cells.[28,29] Therefore, this study also investigated the role of exosomes in melatonin-inhibited metabolic inflammation of adipose tissue to provide potential therapeutic applications.

Adipocytes and macrophages coordinate to preserve tissue integrity while adapting to the metabolic stress in the adipose tissue of obese animals. Numerous studies indicate obesity is associated with an overall increase in the number of macrophages which formed crown-like structures (CLS) in adipose tissue of both rodents and human.[5,30] The combination of an increase in total macrophages and an increased ratio of M1 to M2 macrophages is a hallmark of the adipose tissue inflammation.[31] Recent studies suggest that melatonin attenuates inflammatory response by modulating nitric oxide and arginine metabolism in macrophages.[2,32,33] Moreover, endogenous metabolites function as sensors to transport intercellular signals and induces secretion of potent pro-inflammatory cytokines that contribute to obesity-associated metabolic inflammation conditions.[7,34,35] Studies suggest that the small molecule metabolite is sufficient to regulate multiple chromatin modifications by ten-eleven translocation (Tet)-dependent DNA demethylation, which contributes to numerous inflammatory gene expression.[36,37] Although several studies reveal melatonin inhibits inflammation in adipose tissue, the effects of melatonin on endogenous metabolites in adipose inflammation are still unknown.

In this study, we investigated the effects of melatonin on metabolites during adipose inflammation. We further determined that melatonin could alleviate adipose inflammation though elevating α-ketoglutarate (αKG) in adipocytes and delivering exosomal αKG to macrophages in mice adipose tissue.

## 2 | MATERIAL AND METHODS

### 2.1 | Animal studies

Six-week-old C57BL/6J background male mice were purchased from the Laboratory animal center of the fourth military medical University (Xi'an, China). The use of the animals and mouse handling protocols was conducted following the guidelines and regulations approved by the Animal ethics committee of Northwest A&F university (Yangling, Shaanxi). Mice were housed as 3 per cage, provided ad libitum with water, and a standard laboratory chow diet. The animal room was maintained constant temperature at 25 ± 1°C and humidity at 55 ± 5%, and 12-hour light/dark cycles (24-h LD cycle). Zeitgeber time (ZT) 0 corresponds to the time of light onset. The jet-lagged mice model was constructed as previously described.[26,38] In brief, mice were transferred between two rooms (Room 1: 6:00 AM to 6:00 PM light/6:00 PM to 6:00 AM dark, and Room 2: 10:00 AM to 10:00 PM dark/10:00 PM to 10:00 AM light). Mice were transferred once from room 1 to 2 and then returned to room 1. The time of mice transfer occurs between 9:30 AM and 10:00 AM, leading to an 8-hour phase advance from room 1 to 2 (light off at ZT4 instead of ZT12 for jet-lagged mice on the day of transfer) and an 8-hour phase delay from room 2 to 1 (light off at ZT20 instead of ZT12 for jet-lagged mice on the day of transfer) every 2 days for 14 days. For the lipopolysaccharide (LPS) challenged experiment in vivo, mice were challenged via intraperitoneal (ip) injection with the indicated quantities of LPS (75 μg/kg, Sigma-Aldrich, St. Louis, MO, USA) in PBS for 24 hours.[39] For diet-induced obese mice model, mice were placed on a high-fat diet (HFD, fat provided 60% of the total energy, Trophic animal feed high-tech co., Ltd, Nantong, China) for 10 weeks, and the control mice were fed a standard diet (Chow, fat provided 10% of total energy, Trophic animal feed high-tech co., Ltd). Melatonin injection was performed from then on at a dose of 20 mg/kg/d for 14 days continually.

The melatonin treatment and α-ketoglutarate (αKG) treatment were further applied to HFD fed mice or LPS-treated mice. Melatonin (Sigma-Aldrich) was first dissolved in

amount of absolute ethanol at a final concentration of 0.5% (v/v) ethanol with melatonin and prepared as the stock melatonin solution. Separate experiments showed that there were no additional effects of the melatonin vehicle (0.05% ethanol) on any of the parameters investigated (data not shown). Mice (n = 24) were randomly divided into four groups (n = 6 each). One group of mice received a daily intraperitoneally (IP) injection of a 200 μL solution consisting melatonin (MT, 20 mg/kg) in phosphate-buffered saline (PBS) before the dark onset for 14 days; one group of mice was given a vehicle consisting of a solution of 0.5% ethanol in PBS; one group of mice was administered of αKG (Sigma-Aldrich) at a dose of 2 g/kg body weight by means of an intragastric tube for 14 days; one group of mice received of both melatonin and αKG treatments for 14 days. Jet-lagged mice were pretreated with chronic jet lag for 2 weeks before the melatonin injection experiment. Mice were sacrificed by overdosed ethyl ether within 2 hours after the last injection of melatonin or the vehicle. Immediately, the epididymal white adipose tissue (eWAT) was dissected and kept for the studies as following.

The eWAT and liver tissues were collected immediately and fixed in 4% paraformaldehyde in phosphate buffer. After 2 weeks of incubation, the samples were embedded in paraffin and sectioned. The tissue sections were used for hematoxylin and eosin (H&E) staining. The images were photographed by Cytation 3 cell imaging multimode reader (BioTek, Winooski, VT, USA). Serum aspartate transaminase (AST) and alanine aminotransferase (ALT) levels were measured by the AST and ALT activity assay kits from Sigma (Sigma-Aldrich, MAK055, MAK052). Serum and cell tumor necrosis factor α (TNFα) and interleukin 6 (IL-6) levels were measured by commercial ELISA kits from Sigma (Sigma-Aldrich, RAB0477, RAB0308). Interleukin-1β (IL-1β) level was measured by Mouse IL-1 beta ELISA Kit from Abcam (Cambridge, UK, ab100704). The citrate, malate, fumarate, and αKG levels of eWAT were analyzed using the commercial assay kits from Sigma (Sigma-Aldrich, MAK057, MAK067, MAK060, MAK054) following the manufacturer's instructions.

## 2.2 | Primary cell culture

Primary adipocytes culture was performed as previously described.[26] In brief, eWAT was dissected from mice, washed with PBS, and minced. Pre-adipocytes were seeded onto 35-mm culture dishes at 30% (v/v) confluence, and incubated at 37°C under a humidified atmosphere of 5% $CO_2$ and 95% air for subsequent experiments. After reaching 95% confluence, pre-adipocytes were induced to differentiate using Dulbecco's modified eagle media/nutrient mixture F12 (DMEM/F12; Gibco, Grandland, NY, USA, 12500062) with 10% fetal bovine serum (FBS) and 100 nmol/L insulin for 5-6 days until exhibiting a massive accumulation of fat droplets. Melatonin (MT, Selleck.cn, Shanghai, China) was added into culture medium at a final concentration of 1 μmol/L for 24 hours. αKG (Sigma-Aldrich, 75890) was added into culture medium at a final concentration of 5 mmol/L for 24 hours. For vectors infection study, adipocytes were infected with overexpression adenovirus or interference lentiviral recombinant vectors of sirtuin 1 (*Sirt1*; pAd-*Sirt1* or si-*Sirt1*) or *Mitochondrial isocitrate dehydrogenase 2* (*Idh2*; pAd-*Idh2* or si-*Idh2*) for 48 hours at the titer of $1 \times 10^9$ IFU/mL, and then treated with melatonin or αKG. The control vectors were pAd-GFP or pGLVU6-GFP. All the vectors were constructed by Gene Pharma (Shanghai, China).

Primary peritoneal macrophages were obtained from C57BL/6J mice at 2-3 days after injection of 2 mL of 4% sterile thioglycolate solution as previously described by pelvic washing with PBS containing 3% FBS.[40,41] Primary cultures of macrophages were maintained in RPMI 1640 medium. All culture media were supplemented by addition of 10% FBS and penicillin/streptomycin.

## 2.3 | IDH2 activity measurement

Activity of IDH2 was measured by the Someya method.[42] In brief, 180 μL of the supernatants from homogenized mitochondrial pellets was added in each well of a 96-well plate, and then 180 μL of a reaction mixture (40 mmol/L Tris buffer, 2 mmol/L $NADP^+$, 2 mmol/L $MgCl_2$, and 5 mmol/L isocitrate) was added in each well. The absorbance was immediately read at 340 nm every 10 seconds for 1 minutes in a microplate reader (PerkinElmer Victor X, Waltham, MA, USA). The reaction rates were calculated, and the IDH2 activity in the sample was defined as the production of 1 mmole of NADPH per seconds.

## 2.4 | Plasmid transfection and dual-luciferase reporter assay

A 850 bp mouse *Idh2* promoter was cloned by PCR amplification of C57BL/6J mouse genomic DNA and inserted into the pGL-3 basic vector. The resulting reporter was named $Idh2_{850}$-Luc. Further deletion and relegation of the *Idh2*-Luc generated $Idh2_{540}$-Luc and $Idh2_{360}$-Luc reporters contained of 540 and 360 bp of *Idh2* promoter, respectively. Mutant *Idh2* reporter plasmids were generated using the $Idh2_{540}$-Luc plasmid as a template; a mutagenesis kit (Invitrogen, Carlsbad, CA, USA) was used to created $Idh2_{540}$-$Luc_{E1}$, $Idh2_{540}$-$Luc_{E2}$, and $Idh2_{540}$-$Luc_{E1, E2}$ with mutation in the two E-boxes of *Idh2* promoter. HEK293 cells were co-transfected with luciferase reporter plasmid using X-tremeGENE™ transfection reagent (Roche, Basel, Switzerland), and the same amounts of reporter and β-gal expression vectors, variable amounts of expression vector (pcDNA3.1-*Clock*), and an empty

pcDNA3.1 vector to normalize the total amount DNA. After transfection 48 hours, cells were harvested for luciferase assay, and β-gal was used as an internal control.[26,38]

## 2.5 | Exosome isolation and transmission electron microscopy (TEM) examination

To isolate the exosome, eWAT of mice was washed with Earle's balanced salts (EBSS) and cut into small pieces (1 $mm^3$) then transferred to 90-mm culture dishes containing 10 mL of complete DMEM/F12 medium (Gibco, 12500062) supplemented with 1% antibiotics and 10% FBS that had been depleted of bovine exosomes by overnight ultracentrifugation at 100 000 *g*.[43] The tissues were cultured at 37°C under a humidified atmosphere of 5% $CO_2$ and 95% air for up to 24 hours, and then the conditioned medium samples were collected for exosome purification using differential centrifugation and sucrose density gradient ultracentrifugation. The isolation procedures were all performed at 4°C. The cultured supernatants were centrifuged at 2500 *g* for 20 minutes and then at 10 000 *g* for 30 minutes to remove tissue debris and aggregates. The supernatants were then subjected to 0.22-μm filtration (Millipore, Billerica, MA, USA) and ultracentrifuged at 100 000 *g* for 2 hours. Pelleted vesicles were suspended in 2 mL 1 × PBS and overlaid with 5 mL each of 20% and 40% (w/v) sucrose gradient and ultracentrifuged again at 110 000 *g* for 5 hours. Harvest discontinuous (step) gradient by aspirating the density interface. To remove sucrose, transfer the collected exosomal fractions to a new tube with PBS, and centrifuge 2 hours at 110 000 × *g*, resuspended in 1× PBS, and prepared for electron microscopy detection and diameter measurement.[44,45]

Isolated exosomes were analyzed per duplicate by transmission electron microscopy (TEM). Vesicles were fixed with 4% paraformaldehyde at room temperature for 10 minutes and then layered on carbon/formvar film-coated grids for 10 minutes. After removing sample excess, negative staining was performed by incubation with phosphotungstic acid for 45 seconds. After washing, grids were dried overnight at room temperature. Samples were observed with a transmission electron microscopy (TEM, HT7700, 80 kV, Hitachi, Tokyo, Japan) working at 80 kV. The image calculation was analyzed using Image J software (NIH).

## 2.6 | Co-immunoprecipitation (Co-IP) analysis

HEK293 cells were transfected with plasmids using X-tremeGEN™ transfection reagent (Roche, 06366236001) as previously described.[26] In brief, cells were then snap frozen in lipid nitrogen after 24-hours transfection. Whole cell lysate was harvested in lysis buffer with a protease inhibitor. Cells were then sonicated for 10 seconds, and the whole cell lysate was precleared with protein A for 2 hours and incubated with 2 μg primary antibody overnight at 4°C. Immune complexes were pulled down with protein A agarose for 2 hours at 4°C with shaking. Beads were washed once with lysis buffer and three times with wash buffer, and then eluted by boiling in SDS sample buffer followed detected by western blot.

## 2.7 | Immunocytochemical staining

DNA methylation at the 5-position of cytosines (5mC) represents an important epigenetic modification. 5mC can be converted to 5-hydroxymethylcytosine (5hmC) in an enzymatic process involving members of the TET protein family.[46,47] We then conducted 5-hydroxymethylcytosine (5hmC) immunocytochemical staining using method from Yang to show the epigenetic status.[48] Cells grown on 24-well plates were incubated in cold methanol for 10 minutes, and permeabilized with PBS containing 0.25% Triton X-100 for 10 minutes. After blocking 1 hour with 1% BSA, cells were incubated with 5hmC antibody (1:50; Cell Signaling Technology, Boston, MA, USA, #51660) at 4°C overnight. After washing for 3 times, fluorescent secondary antibody (1:1000) was then added for 1 hour. Fluorescence was examined using a Cytation 3 cell imaging multimode reader (BioTek, VT). To quantitate 5hmC levels in representative images, the images were analyzed using the Image J software (NIH) application. To account for differences in differences in overall DNA content, 5hmC signal intensities were normalized to DAPI intensities.

Paraffin-embedded eWAT was sectioned, dewaxed, and rehydrated prior to antigen retrieval by boiling in 10 mmol/L sodium citrate buffer (pH 6.5). Tissue samples were blocked with 5% normal rabbit serum for 40 minutes, followed by incubation for 2 hours with 10 μg/mL F4/80 antibody (Abcam, Cambridge, UK, ab6640). And then incubated with fluorescein isothiocyanate-conjugated goat against rabbit IgG antibody (Boster, China; diluted 1:100) for 1 hour at room temperature. After washing for 3 times, the nuclei were stained with DAPI for 5 minutes. Average numbers of F4/80-positive cells in the slides were calculated by scoring five random 200× microscopic fields of stained adipose tissue sections of each mouse using a Cytation 3 cell imaging multimode reader (BioTek, VT).

## 2.8 | RNA extraction and Real-time PCR

Total RNA of eWAT or adipocytes was extracted with TRIpure Reagent kit (Takara, Dalian, China). 500 ng of total RNA was reverse transcribed using M-MLV reverse transcriptase kit (Takara). Primers were synthesized by Invitrogen (Shanghai, China). Real-time PCR was performed in 25 μL reaction system containing specific primers and AceQ qPCR SYBR Green Master Mix (Vazyme Biotech,

Nanjing, China). Amplification was performed in the ABI StepOne plus™ RT-PCR System (Carlsbad, CA, USA). The levels of mRNA were normalized in relevance to *Gapdh*. The expression of genes was analyzed by method of $2^{-\Delta\Delta C_t}$.

## 2.9 | Immunoblotting analyses

Protein was isolated from tissues or cultured cells. Western blot was performed as previously described.[26] Protein samples (30 μg) were separated by electrophoresis on 12% and 5% SDS-PAGE gels using slab gel apparatus, and transferred to PVDF nitrocellulose membranes (Millipore). Antibodies, including FLAG-HRP (A-8592, Sigma-Aldrich), Anti-His tag (ab18184, Abcam), anti-CD9 (ab92726), anti-CD81 (#10037, Cell Signaling Technology), anti-STAT3 (ab68153), anti-p-STAT3 (ab76315), anti-NF-κB (ab207297), anti-p-NF-κB (ab222494), anti-Cyt C (ab133504), anti-GAPDH (AP0063, Bioword, China), anti-β-actin (AP0060, Bioworld, Nanjing, China), anti-Cd11c (#435421, R&D system), anti-TNFα (ab6671), anti-Cd206 (AF2535, R&D system), anti-CD163 (NBP2-36494, Novus Biologicals, Littleton, CO, USA), anti-Tet1 (ab191698), anti-Tet2 (ab94580), anti-Tet3 (ab139311), anti-DNMT1 (ab19905), anti-DNMT2 (ab71015), and the appropriate HRP-conjugated secondary antibody (Baoshan, China) were used. Proteins were visualized using chemiluminescent peroxidase substrate (Millipore), and then the blots were quantified using ChemiDoc XRS system (Bio-Rad, Richmond, CA, USA).

## 2.10 | Statistical analysis

Statistical analyses were conducted using SAS v8.0 (SAS Institute, Cary, NC, USA). Data were analyzed using one-way ANOVA and two-way ANOVA. Comparisons among individual means were made by Fisher's least significant difference (LSD). Data were presented as mean ± SEM. $P < .05$ was considered to be significant.

# 3 | RESULTS

## 3.1 | Melatonin increases αKG level in obesity-induced adipose inflammation

To explore the effects of melatonin on adipose inflammation, we first placed mice on high-fat diet (HFD) and then treated mice with melatonin. H&E staining showed melatonin significantly reduced adipocyte size both in the chow diet group and in the HFD group (Figure 1A). Compared with chow diet group, the mRNA levels of inflammation indicators, such as *tumor necrosis factor* α (*TNF*α), *interleukin 6* (*IL-6*), and *interleukin-1*β (*IL-1*β), were all increased markedly with HFD; while melatonin injection alleviated this chronic inflammation caused by

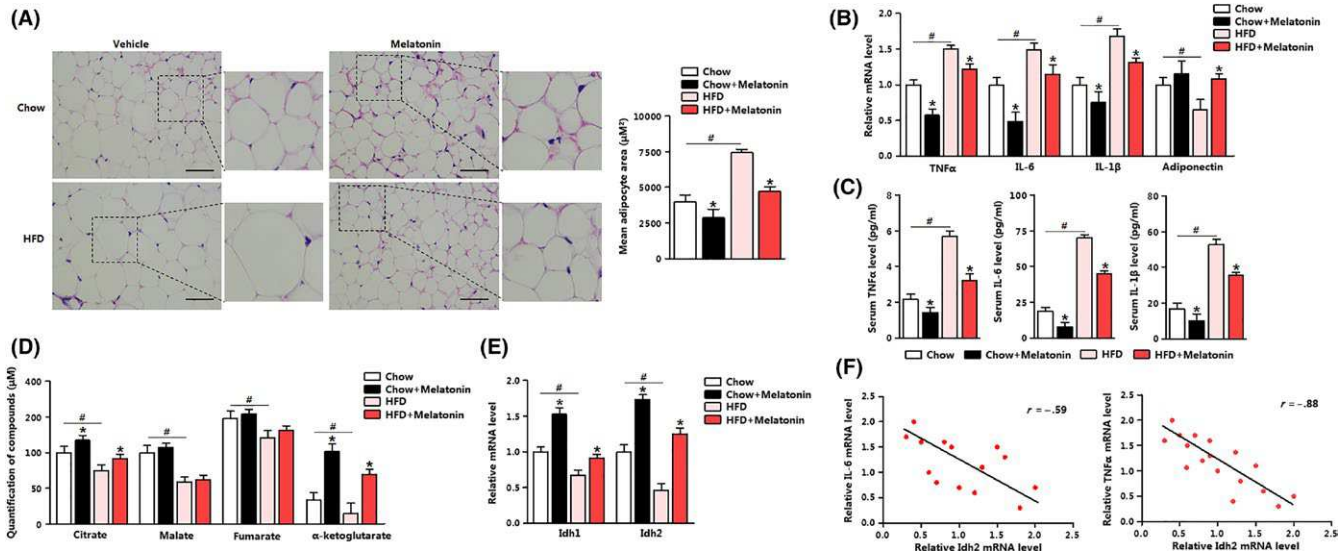


**FIGURE 1** Melatonin increases αKG level in obesity-induced adipose inflammation. (A) Representative hematoxylin and eosin (H&E) staining of adipose sections from high-fat diet (HFD) or chow diet mice treated with melatonin or not. The small images on the right side were the expansion (n = 6). (B) mRNA levels of inflammation marker genes with or without melatonin treatment of HFD and chow diet mice (n = 6). (C) Serum levels of tumor necrosis factor α (TNFα), interleukin 6 (IL-6), and interleukin-1β (IL-1β) of HFD and chow diet mice treated with melatonin or not (n = 6). (D) Concentration of key metabolites of the tricarboxylic acid (TCA) cycle of HFD and chow diet mice treated with melatonin or not (n = 6). (E) mRNA levels of isocitrate dehydrogenase 1 (*Idh1*) and *isocitrate dehydrogenase 2* (*Idh2*) of HFD and chow diet mice treated with melatonin or not (n = 6). (F) Regression analysis of *Idh2* and *interleukin-6* (*IL-6*) of mice adipose tissue (n = 6). Protein level was detected by ELISA method. Values are means ± SEM. *$P < .05$ compared with the control group

obesity (Figure 1B). Further protein level detection by ELISA method confirmed that TNFα, IL-6, and IL-1β were all reduced by melatonin (Figure 1C). Metabolic analyses by ELISA method identified metabolite contents such as citrate and αKG were increased due to melatonin injection in HFD group; but the contents of malate and fumarate were comparable (Figure 1D). Next we analyzed the mRNA level of rate-limiting enzymes which catalyzing αKG generation. During melatonin treatment in HFD mice, the mRNA level of *isocitrate dehydrogenases* (*Idh*) was dramatically increased, especially *Idh2*, suggesting melatonin regulate adipose metabolism via *Idh2* (Figure 1E). As expect, correlation analysis showed both the expressions of *IL-6* and *TNF*α were negatively correlated with *Idh2* (Figure 1F). These data suggest melatonin involved in adipose inflammation and increased αKG level of adipose tissue.

### 3.2 | Melatonin and αKG coordinately reduces adipose inflammation in LPS-challenged mice

With H&E staining, we found that the density of crown-like structures (CLS) was much lower in αKG and melatonin separately treated mice compared with that of control mice which had been pretreated with lipopolysaccharide (LPS; Figure 2A). Furthermore, αKG and melatonin co-treatment group contained lowest density of CLS (Figure 2A). Consistently, gene expression analysis showed *TNF*α, *IL-6,* and *IL-1*β were reduced due to the treatment of melatonin and αKG in LPS-pretreated mice (Figure 2B). ELISA measurement further showed serum TNFα, IL-6, and IL-1β levels were reduced with αKG and melatonin co-treatment (Figure 2C). αKG had no effect on IDH2 activity, while melatonin injection increased IDH2 activity drastically, and it also happened in the co-treatment group using ELISA

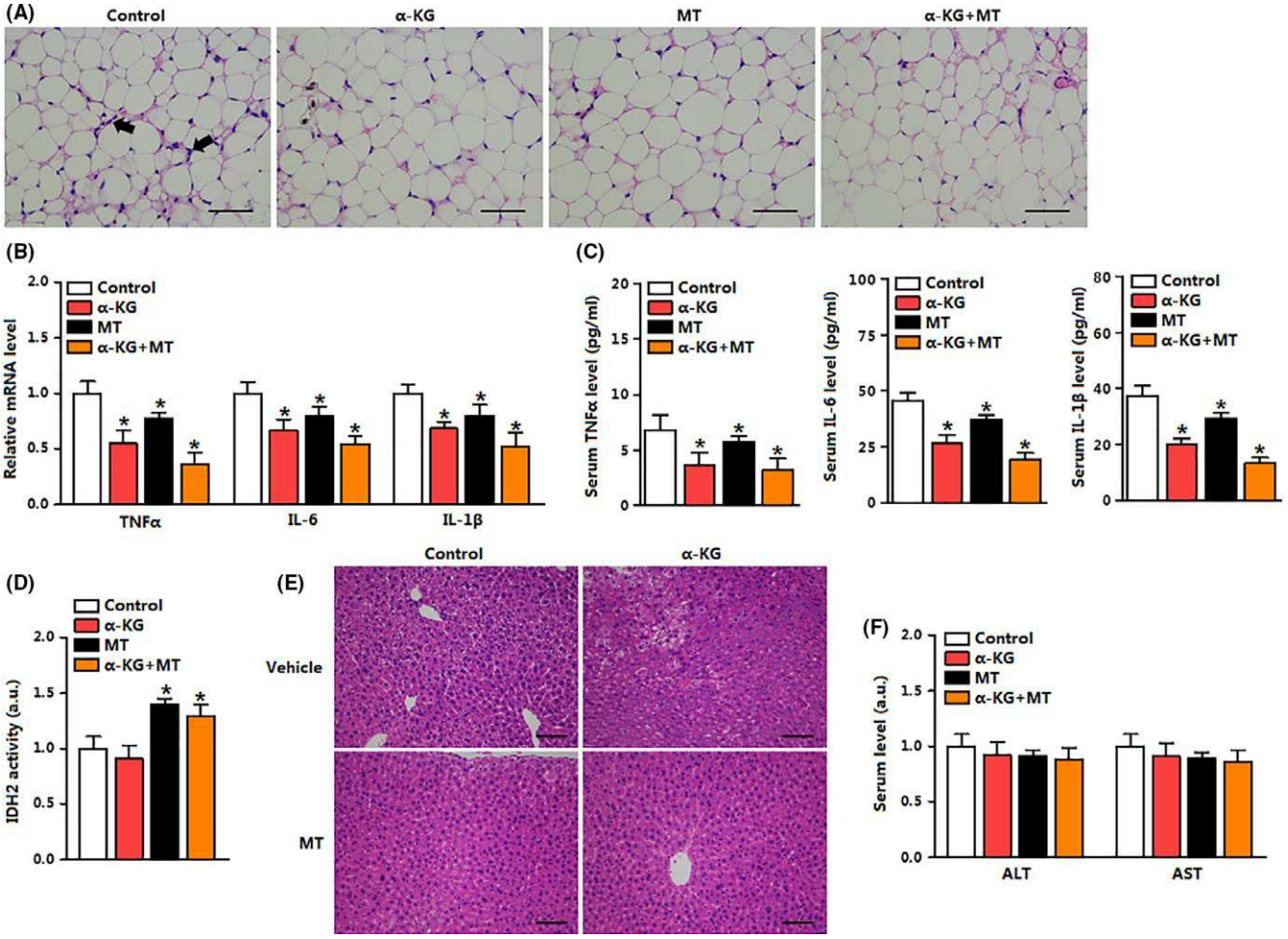


**FIGURE 2** Melatonin and αKG coordinately reduce adipose inflammation in LPS-challenged mice. All the experiments were performed in LPS-challenged mice. (A) Representative H&E staining of adipose sections treated with melatonin or αKG. Black arrows: crown-like structures (CLS). Scale bar: 200 μm (n = 6). (B) mRNA levels of inflammation indicators of mice adipose treated with melatonin or αKG (n = 6). (C) Serum levels of TNFα, IL-6, and IL-1β of mice treated with melatonin or αKG (n = 6). (D) IDH2 activity of mice adipose treated with melatonin or αKG (n = 6). (E) Representative H&E staining of liver sections treated with melatonin or αKG. Scale bar: μm (n = 6). (F) Serum levels of alanine aminotransferase (ALT) and aspartate transaminase (AST) of mice treated with melatonin or αKG (n = 6). Protein level was detected by ELISA method. Values are means ± SEM. **P* < .05 compared with the control group

detection (Figure 2D). Moreover, H&E staining demonstrated liver morphology and liver metabolic were unaltered in αKG and melatonin-treated mice (Figure 2E,F). In short, melatonin and αKG alleviate the induction of adipose tissue inflammation.

### 3.3 | Melatonin enhances DNA demethylation of mice adipocytes

As shown in Figure 3A, RNA-seq analysis indicated melatonin treatment drastically increased the expression of genes involved in TCA cycle (Figure 3A,B). The mRNA expression measurement established that *fumarate hydratase 1* (*FUM1*), *Idh1,* and *Idh2* were increased with melatonin incubation of adipocytes (Figure 3C). We also confirmed that melatonin significantly increased the levels of melatonin receptor 1 and 2 (MT1 and MT2; Figure 3C). The in vitro study in adipocytes further demonstrated that melatonin treatment increased the content of αKG and elevated IDH2 activity (Figure 3D,E). Additionally, melatonin increased the mRNA expression level of *ten-eleven translocation 2* (*Tet2*) and *ten-eleven translocation 3* (*Tet3*) but not *ten-eleven translocation 1* (*Tet1*), showing the enhancement of DNA demethylation

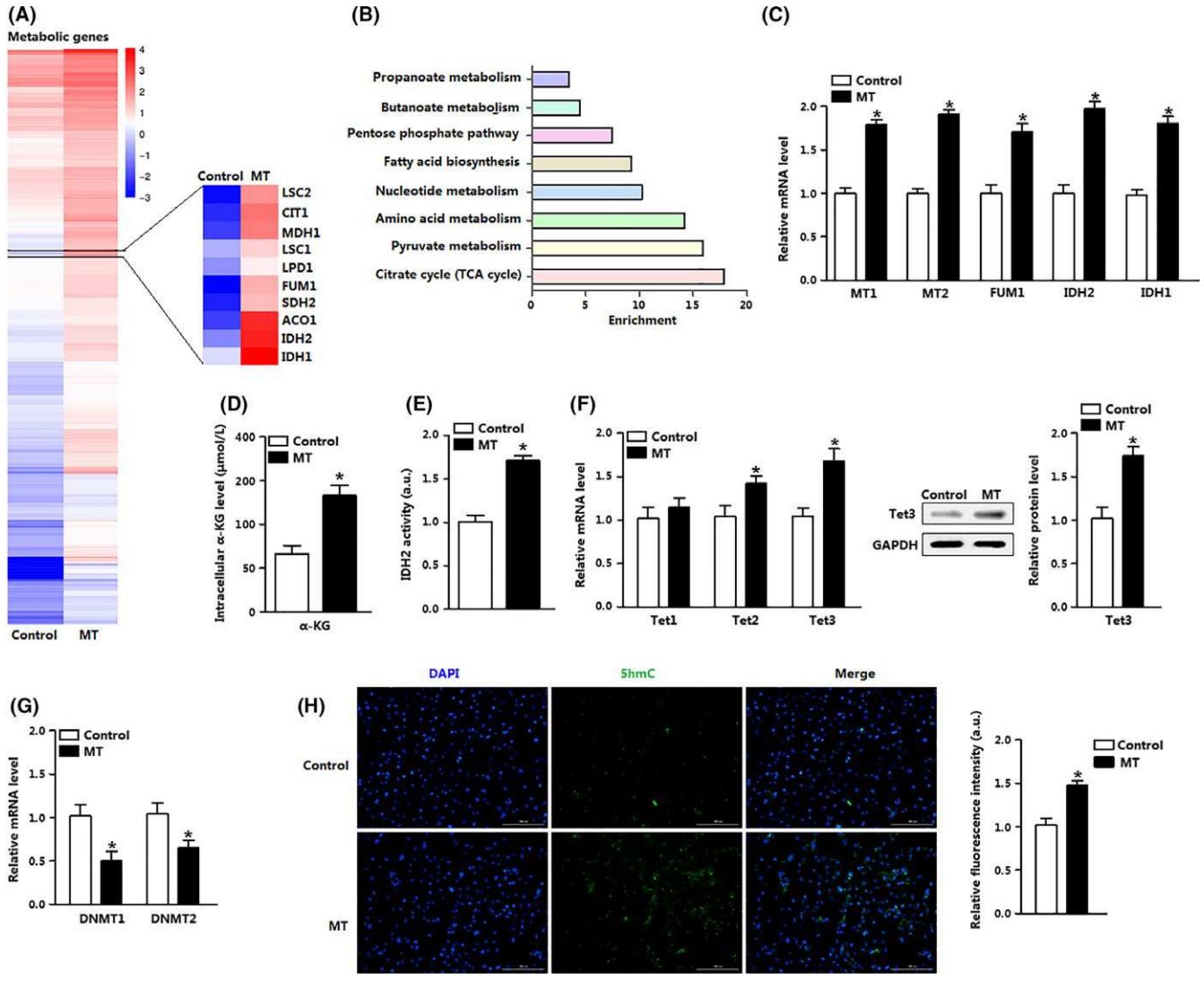


**FIGURE 3** Melatonin enhances DNA demethylation of mice adipocytes. (A) Heatmap of genes upregulated or downregulated with melatonin treatment of mice adipocytes, along with the top affected genes with melatonin treatment (n = 3). (B) Gene ontology (GO) analysis of the target genes in Figure 1A, showing the biology process for melatonin treatment (n = 3). (C) mRNA levels of *melatonin receptor 1* and *2* (*MT1* and *MT2*), *fumarate hydra-tase 1* (*Fum1*), *Idh1,* and *Idh2* of adipocytes treated with melatonin (n = 3). (D) Concentration of αKG of adipocytes treated with melatonin (n = 3). (E) IDH2 activity of adipocytes treated with melatonin (n = 3). (F) mRNA levels of *ten-eleven translocation 1* (*Tet1*) and *ten-eleven translocation 2* (*Tet2*) of adipocytes treated with melatonin. Right panel: protein level of Tet3 of adipocytes treated with melatonin (n = 3). (G) mRNA levels of *DNA methyltransferase 1* (*DNMT1*) and *DNA methyltransferase 2* (*DNMT2*) of adipocytes treated with melatonin (n = 3). (H) Immunohistochemical staining of 5-hydroxymethylcytosine (5hmC) of adipocytes treated with melatonin. Scale bar: 200 μm (n = 3). Values are means ± SEM. **P* < .05 compared with the control group

(Figure 3F). The protein level of Tet3 was also elevated with melatonin incubation (Figure 3F). The expression of *DNA methyltransferase 1* (*DNMT1*) and *DNA methyltransferase 2* (*DNMT2*) was accompanied decreased (Figure 3G). In agreement, the enrichment of 5hmC from immunocytochemical staining measurement was also enhanced with melatonin incubation (Figure 3H). Thus, these data suggest melatonin promotes the production of αKG, thereby increasing DNA demethylation of adipocytes.

### 3.4 | Sirt1 and IDH2 formed a complex to increase αKG level

We then questioned how melatonin upregulated the level of αKG. In fact, studies have demonstrated melatonin directly regulated Sirt1;[49] and firstly based on the bioinformatics analysis and previous data sheet, our study showed Sirt1 interacted with IDH2 on protein level (Figure 4A). Then by protein-protein measurement, data indicated Sirt1 protein interacted strongly with transfected IDH2 in HEK293 cells (Figure 4B). We then overexpressed *Sirt1* in adipocytes and with the incubation of melatonin, we found the level of αKG was drastically enhanced; while knock down of *Sirt1* obtained the opposite results (Figure 4C). Moreover, melatonin along with pAd-*Sirt1* infection further reduced *IL-6* expression (Figure 4D). We then confirmed the reduction of inflammation by measuring the protein levels of TNFα, IL-6, and IL-1β by ELISA in adipocytes treated with MT and pAd-*Sirt1* (Figure 4E). Thus, these data suggest that Sirt1 and IDH2 directly bind, and then regulated αKG level in adipocytes; melatonin functioned via the direct modification between Sirt1 and IDH2.

### 3.5 | Exosomal αKG promotes M2 macrophage activation and enhances DNA demethylation

To determine whether the metabolite from adipose-derived exosome contributed to adipose inflammation, we isolated exosomes from the eWAT of mice pretreated with melatonin ($Exos_{MT}$) by differential ultracentrifugation (Figure 5A). Analyze revealed that these vesicles were 20-70 nm in diameter (Figure 5B) and positively immunereactive to exosomal markers CD9 and CD81 from Western blot measurement (Figure 5C). Electron microscopy images confirmed that exosomes were clearly separated and the size was consistent with diameter measurement (Figure 5D). And with melatonin treatment, αKG level from adipose-derived exosome was increased (Figure 5E).

To verify that exosomes derived from melatonin-treated adipose tissue affected the macrophage population, we co-cultured macrophages with adipose tissue-derived exosomes for 24 hours. Interestingly, $Exos_{MT}$ treatment significantly increased αKG level of macrophages which is similarly to αKG-treated group (Figure 6A). $Exos_{MT}$ treatment also elevated the expression of *OXGR1*, the receptor of αKG (Figure 6B). In addition, the percentage of M2 macrophage was higher in $Exos_{MT}$ group than that in the control group from microscopy images (Figure 6C), and consistent results were observed in the αKG-treated group. Increased levels of specific M2 macrophage markers have been found with $Exos_{MT}$ incubation, with decreased of M1 macrophage indicators both on mRNA level and on protein level (Figure 6D,E). To understand more clearly about the correlation of $Exos_{MT}$ and αKG in macrophages, we then measured the DNA demethylation of macrophages. As shown in Figure 6F–I, αKG significantly enhanced the mRNA levels and protein levels of Tet1, Tet2, and Tet3, and reduced DNMT1 and DNMT2. And $Exos_{MT}$ treatment showed enhanced DNA demethylation either (Figure 6F–I). The enrichment of 5hmC in both αKG group and $Exos_{MT}$ group further confirmed the elevation of DNA demethylation (Figure 6J). These data clearly indicate adipose tissue-derived exosomes, similarly as αKG, increase M2 macrophage and enhance DNA demethylation in macrophages, verify the correlation between adipocytes and macrophages.

### 3.6 | Adipose-derived exosomes inactivate STAT3/NF-κB signal in adipocytes

We next explore the function of exosomes derived from melatonin-treated adipose tissue in adipocytes. Adipocytes were separately incubated with αKG and $Exos_{MT}$. The mRNA level and protein level of TNFα, IL-6, and IL-1β were greatly reduced with αKG incubation, and similarly results were found in $Exos_{MT}$ treatment group (Figure 7A,B). Consistently with the results of macrophages, $Exos_{MT}$ markedly elevated αKG content of adipocytes (Figure 7C). Further measurement showed increasing *oxoglutarate receptor 1* (*OXGR1*) confirmed the elevation of αKG in $Exos_{MT}$ (Figure 7D). In agreement with early study that αKG functioned via the inactivation of STAT3/NF-κB signals in mediating inflammation, our data demonstrated $Exos_{MT}$ also reduced the phosphorylation levels of STAT3 and NF-κB, pointing to the correlation between $Exos_{MT}$ and αKG (Figure 7E). Based on these findings, the effects of $Exos_{MT}$ in alleviating adipose inflammation and enhancing DNA demethylation imply αKG from $Exos_{MT}$ play an important role in the regulation of these processes.

### 3.7 | Melatonin drives circadian amplitude of *Idh2* in adipose inflammation

To further dissect the regulation of melatonin on αKG, we examine the 24-hour mRNA pattern of *Idh2*. Interestingly, the expression profile of *Idh2* showed a circadian rhythm by the cosine method (Figure 8A). And melatonin treatment increased the circadian amplitude of *Idh2* (Figure 8A). Based on our previous study, we firstly considered the gene *Clock*

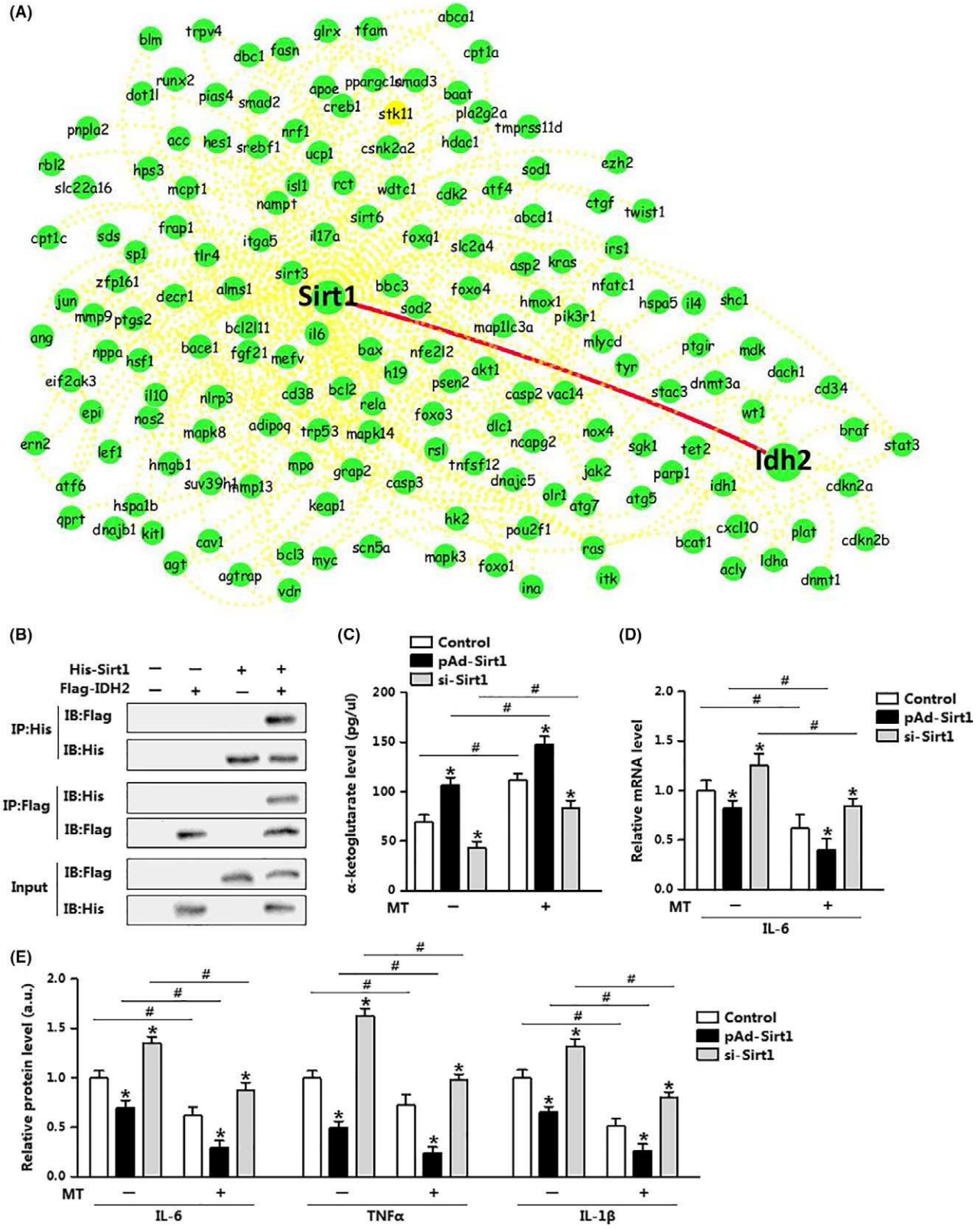


**FIGURE 4** Sirt1 and IDH2 formed a complex to increase αKG level. (A) IDH2 interacted with sirtuin 1 (Sirt1). (B) Co-IP analysis was performed in His-Sirt1 and Flag-IDH2 transfected HEK293 cells (n = 3). (C) αKG concentration of adipocytes pre-infected with pAd-*Sirt1* or si-*Sirt1*, and then treated with or without melatonin (n = 3). (D) mRNA level of *IL-6* of adipocytes pre-infected with pAd-*Sirt1* or si-*Sirt1*, and then treated with or without melatonin (n = 3). (E) Protein levels of TNFα, IL-6, and IL-1β of adipocytes pre-infected with pAd-*Sirt1* or si-*Sirt1*, and then treated with or without melatonin (n = 3). pAd-*Sirt1,* overexpression adenovirus vector of *Sirt1*; si-*Sirt1,* interference lentivirus vector of *Sirt1*. Protein level was detected by ELISA method. Values are means ± SEM. *$P < .05$ compared with the control group, $^{\#}P < .05$ compared with the MT group

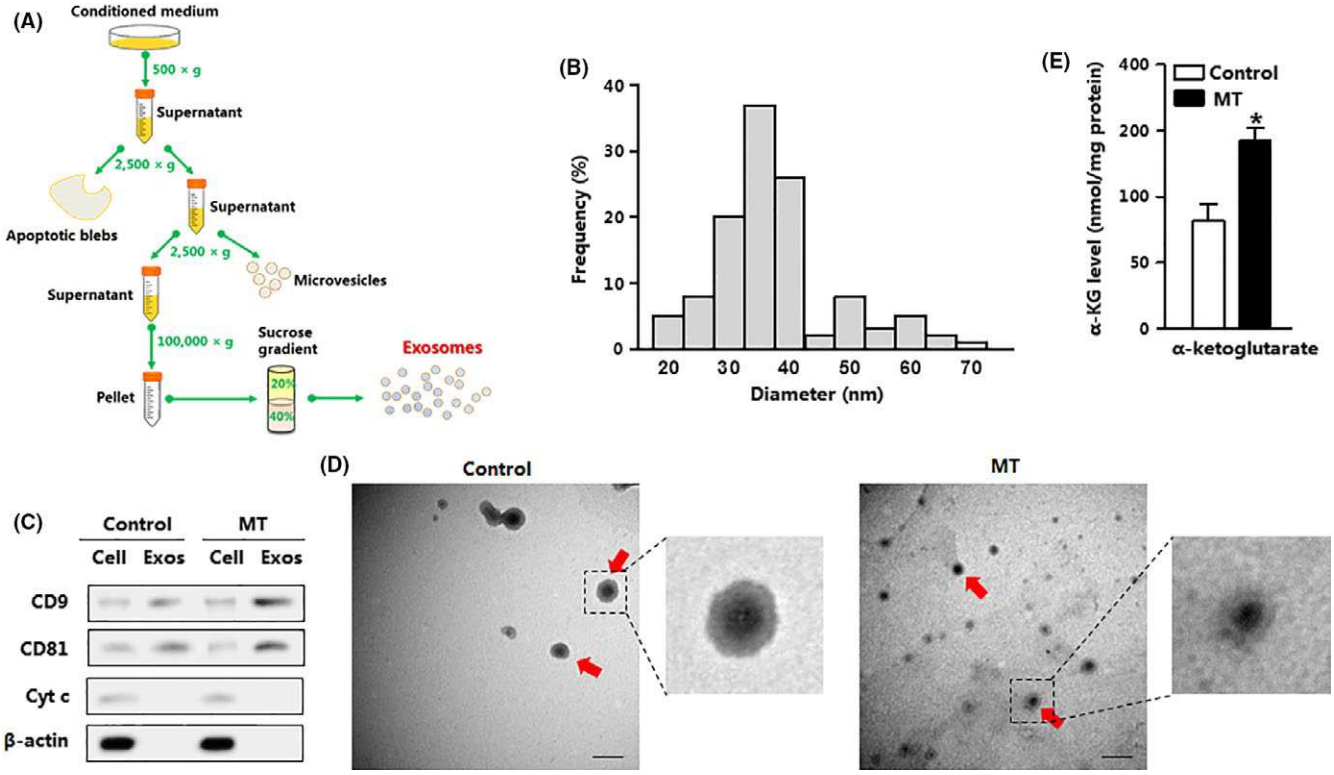


**FIGURE 5** Isolation of exosomes from mice adipose tissue. (A) A schematic depiction of adipose exosome isolation. (B) Size distribution of adipose-derived exosome as showed the peak at 30-40 nm (n = 3). (C) The exosome fractions and cell lysates of adipose-derived exosomes were analyzed by immunoblotting with antibodies against exosomal proteins CD9 and CD81 and cellular proteins Cyt c and β-actin (n = 3). (D) Electron microscopy (EM) images of exosomes. Right panel: the expansion image of the original image. EM scale bar: 100 nm (n = 3). (E) αKG concentration from adipose-derived exosomes treated with or without melatonin (n = 3). Values are means ± SEM. *$P < .05$ compared with the control group

as a key regulator. Dual-luciferase reporter assay demonstrated *Idh2* promoter contained three consensus E-box elements that were the potential targets of *Clock* (Figure 8B). Further measurements revealed that three E-box elements, 850-230 bp upstream of the initiation codon of *Idh2* functioned (Figure 4B). Mutation of the two E-box elements in the *Idh2* promoter impaired the effects of *Clock* on *Idh2* transcription activity (Figure 8C), indicating that both of the two E-box elements regulated the translation of *Idh2*. We then overexpressed *Idh2* in adipocytes with or without melatonin incubation. Co-treatment of *Idh2* and melatonin further elevated the content of αKG, along with the reduction of *IL-6* mRNA level (Figure 8D,E). In addition, ELISA measurement showed co-treatment of *Idh2* and melatonin reduced the protein levels of TNFα, IL-6, and IL-1β (Figure 8F). Thus, these findings suggest *Clock* positively regulates *Idh2* on transcriptional level, and melatonin functioned via the regulation of *Idh2*.

### 3.8 | Melatonin attenuates jet-lagged-induced inflammation in mice adipose tissue

To test the effects of melatonin on circadian misalignment induced adipose inflammation, we used jet-lagged mice model. Melatonin elevated αKG level which had been decreased in jet-lagged mice (Figure 9A). Meanwhile, melatonin promoted IDH2 activity of adipose tissue that was disturbed in jet-lagged mice (Figure 9B). As shown in Figure 9C, melatonin reduced the mRNA levels of *TNF*α and *IL-6* of jet-lagged mice adipose tissue. And immunocytochemical staining showed melatonin decreased the F4/80-positive cells of jet-lagged mice (Figure 9D). Taken together, melatonin reduced adipose inflammation of jet-lagged condition.

## 4 | DISCUSSION

Melatonin is known to function as an immune modulator in obesity and age-related diseases.[50,51] Melatonin exerts its anti-inflammatory effects by controlling the release of various anti-inflammatory and also pro-inflammatory cytokines.[13,18,52] Although studies report that melatonin inhibits inflammatory response via melatonin receptor (MT1) receptor as well as nuclear receptors of ROR family present in immune cells, the effects of melatonin on the communication of adipocytes and macrophages during obesity-associated metabolic inflammation are still not determined.[21,53] In this study, we demonstrated that exogenous melatonin ameliorated

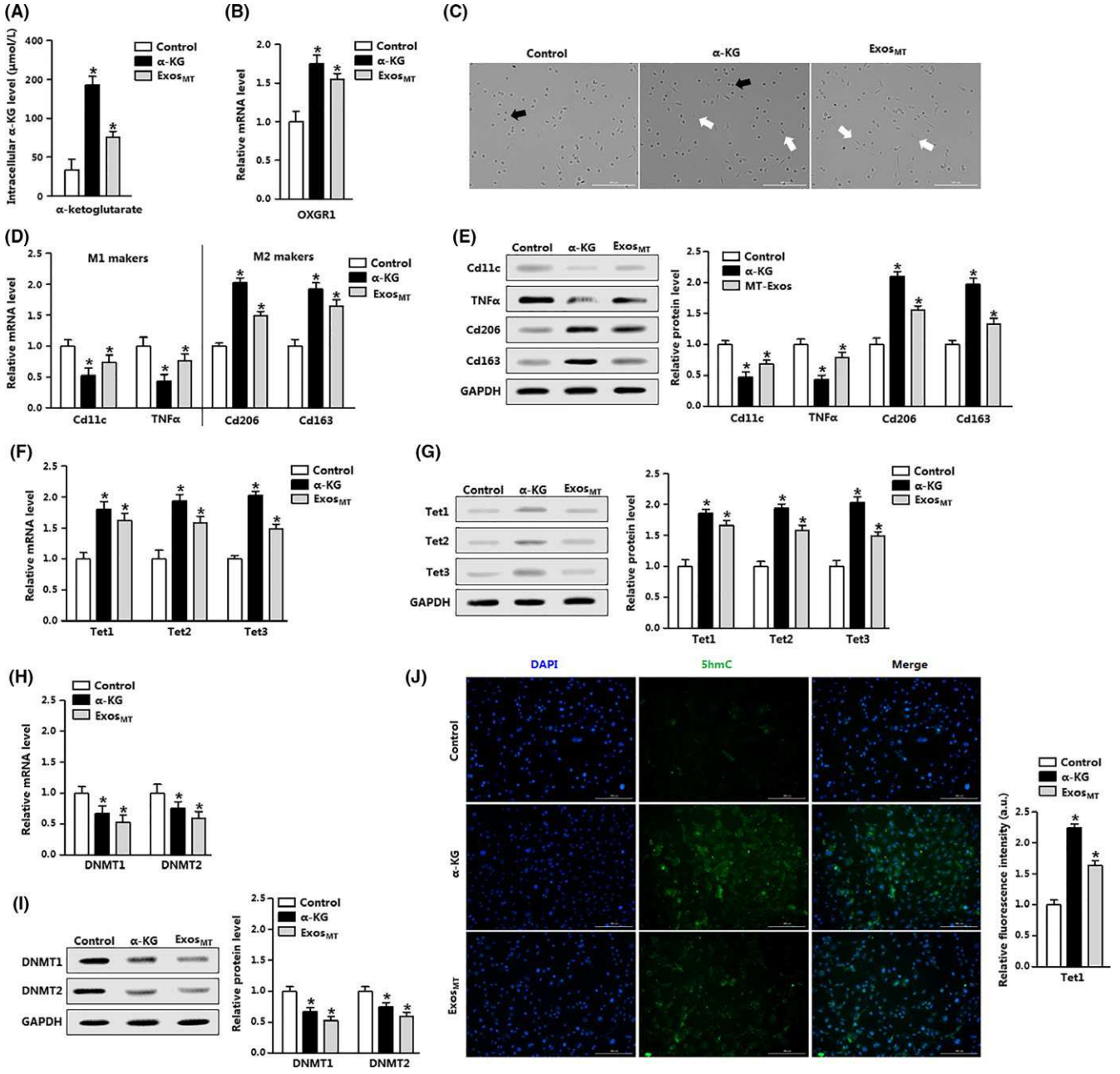


**FIGURE 6** Exosomal αKG promotes M2 macrophage activation and enhances DNA demethylation. Macrophages were pretreated with αKG, adipose-derived exosome (Control), or adipose-derived exosome which had been incubated with melatonin (Exos$_{MT}$). (A) Intracellular αKG level of macrophages (n = 3). (B) mRNA level of *oxoglutarate receptor 1* (*OXGR1*) of macrophages (n = 3). (C) Representative pictures of M1 macrophages and M2 macrophages. Scale bar: 200 μm. Black arrow: M1 macrophage, white arrow: M2 macrophages (n = 3). (D) mRNA levels of M1 and M2 macrophage indicators of macrophages (n = 3). (E) Protein levels of Cd11c, TNFα, Cd206, and Cd163 of macrophages (n = 3). (F) mRNA levels of *Tet1*, *Tet2,* and *Tet3* of macrophages (n = 3). (G) Protein levels of Tet1, Tet2, and Tet3 of macrophages (n = 3). (H) mRNA levels of *DNMT1* and *DNMT2* of macrophages (n = 3). (I) Protein levels of DNMT1 and DNMT2 of macrophages (n = 3). (J) Immunohistochemical staining of 5hmC of macrophages. The right panel was the quantification of fluorescence intensity. Scale bar: 200 μm (n = 3). Values are means ± SEM. **P* < .05 compared with the control group

inflammation of adipose tissue. Considering the similar results in HFD and chow diets, we hypothesized that melatonin might affect important metabolites in both steady and stress state. Recently, studies confirm that the metabolites can contribute to the maintenance of cellular homeostasis and have important roles in inflammation and immune response.[54-56] In addition, we found melatonin also elevated the cellular levels of citrate and αKG in adipose tissue. Thus, our data indicated that αKG might be involved in melatonin reducing inflammatory response of adipose tissue.

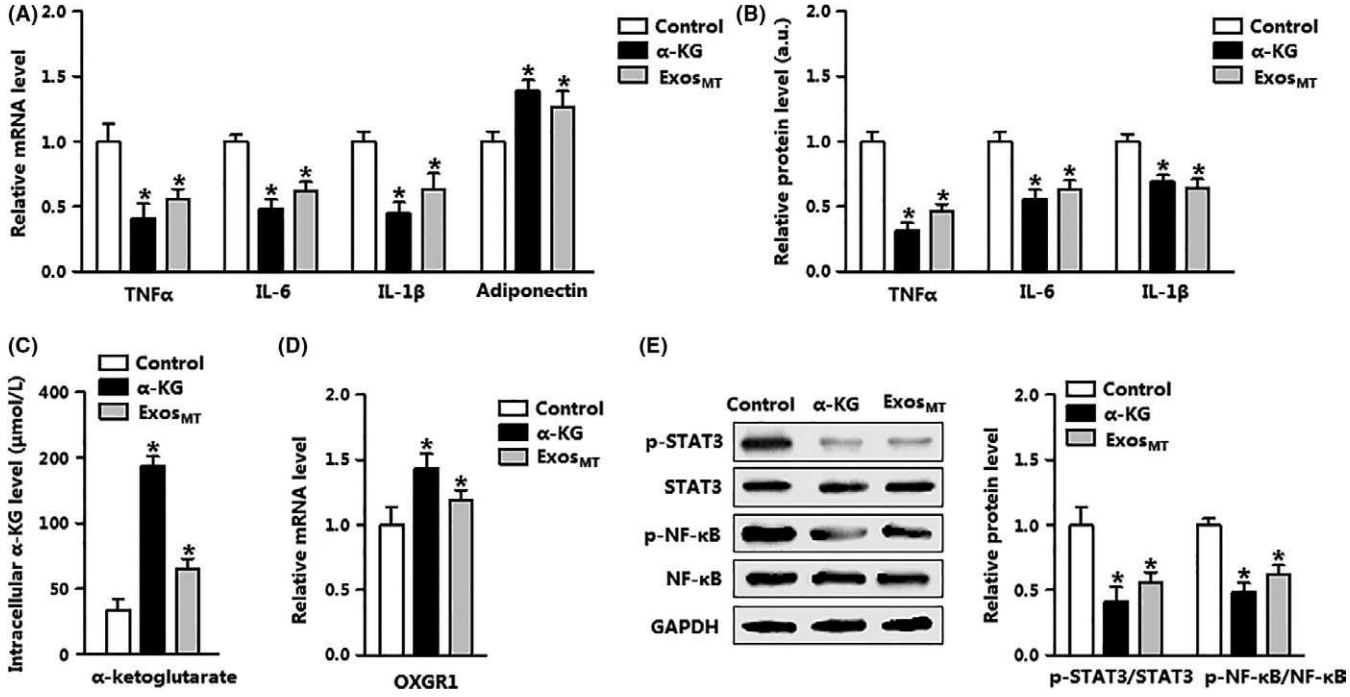


**FIGURE 7** Adipose-derived exosomes inactivate STAT3/NF-κB signal in adipocytes. The adipocytes were pretreated with αKG, adipose-derived exosome (Control), or adipose-derived exosome which had been incubated with melatonin (Exos$_{MT}$). (A) mRNA levels of inflammatory markers of adipocytes (n = 3). (B) Protein levels of TNFα, IL-6, and IL-1β of adipocytes (n = 3). (C) Intracellular αKG level of adipocytes (n = 3). (D) mRNA level of *OXGR1* of adipocytes (n = 3). (E) Protein levels of p-STAT3, STAT3, p-NF-κB, and NF-κB of adipocytes (n = 3). Protein level was detected by ELISA method. Values are means ± SEM. **P* < .05 compared with the control group

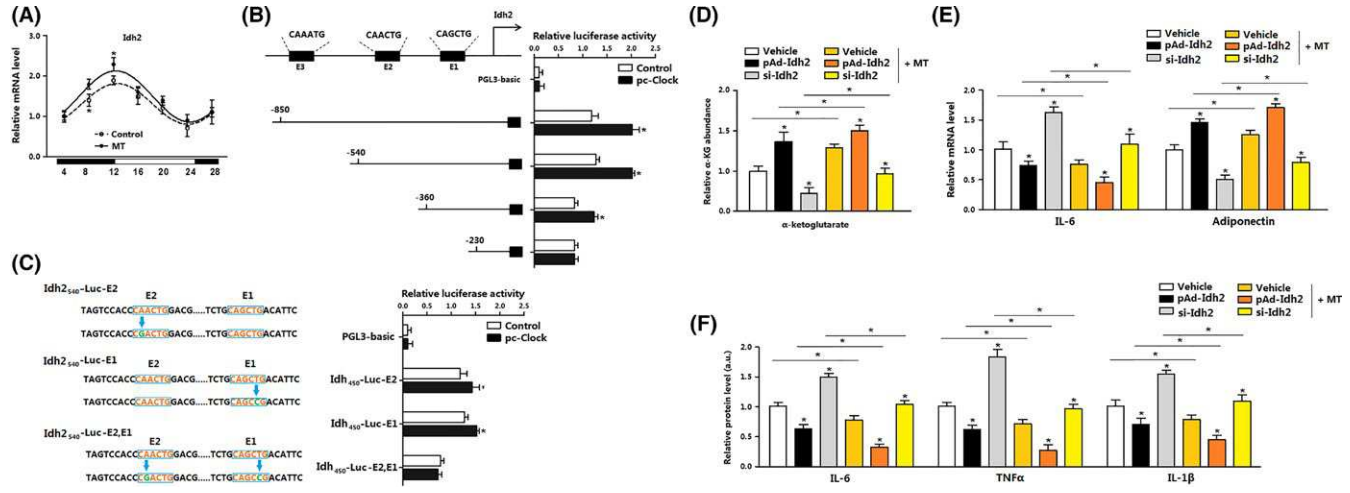


**FIGURE 8** Melatonin drives circadian amplitude of *Idh2* in adipose inflammation, (A) mRNA level of *Idh2* at indicated times was analyzed by RT-PCR (n = 3). (B) Fragments of *Idh2* promoter fused to a luciferase reporter gene were co-transfected into HEK293 cells together with PGL3-basic (control) or pc-*Clock*. The binding sites of Clock overlap with consensus E-boxes in *Idh2* promoter region. Luciferase activity was corrected for Renilla luciferase activity and normalized to the control activity (n = 3). (C) The strategy for generating mutant *Idh2* promoter-driven luciferase reporters with mutated bases in red (n = 3). (D) Relative αKG abundance of adipocytes pre-infected with pAd-*Idh2* or si-*Idh2* and treated with melatonin or not (n = 3). (E) mRNA levels of *IL-6* and *adiponectin* of adipocytes pre-infected with pAd-*Idh2* or si-*Idh2* and treated with melatonin or not (n = 3). (F) Protein levels of TNFα, IL-6, and IL-1β of adipocytes (n = 3). pAd-*Idh2*: overexpression adenovirus recombinant vectors of *Idh2*; si-*Idh2*: interference lentiviral recombinant vectors of *Idh2*. Protein level was detected by ELISA method. Values are means ± SEM. **P* < .05 compared with control

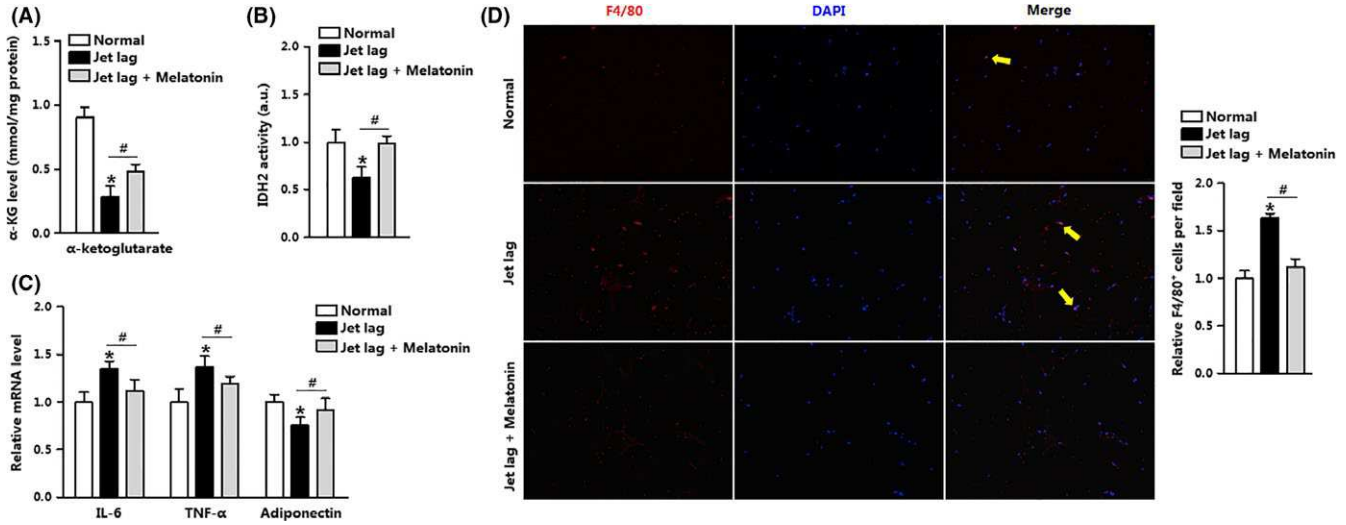


**FIGURE 9** Melatonin attenuates jet-lagged-induced inflammation in mice adipose tissue. The jet-lagged mice were injected with or without melatonin for 14 days, and n = 6 in each group. (A) αKG level of adipose tissue of jet-lagged mice. (B) IDH2 activity of adipose tissue of jet-lagged mice. (C) mRNA levels of *IL-6*, *TNF*α, and adiponectin of adipose tissue of jet-lagged mice. (D) Adipose tissue sections were stained with the macrophage-specific antibody F4/80. The right panel was the quantification of fluorescence. Values are means ± SEM. **P* < .05 compared with control

There exists a substantial amount of evidence supporting that melatonin can accelerate key enzymes of the Kreb's cycle and the respiratory chain. Among the known metabolites, αKG has been reported to be essential for the elicitation of desirable immune responses.[57] Recent studies also confirm that melatonin elevates cellular αKG level and prevents α-ketoglutarate dehydrogenase activation in liver and kidney.[58,59] To estimate the effects of melatonin on cellular αKG level in adipocyte inflammation, we investigated the core metabolic and inflammatory genes expression profile in adipose tissue. We found that melatonin elevated the expression of TCA cycle genes including *Idh1*, *Idh2,* and *Idh3*. Moreover, the NF-κB signal pathway which was correlated with inflammatory responses was significantly enriched by the gene ontology (GO) analysis. Studies have identified that αKG links metabolism to epigenetic modifications in adipocytes differentiation and thermogenesis by TET-mediated DNA demethylation.[48,60] In this study, our data preliminarily showed that melatonin increased cellular αKG level along with the increasing of DNA demethylation during inflammatory response in adipocytes. Furthermore, melatonin could elevate IDH2 activity by Sirt1 directly interaction with IDH2 and suppressed pro-inflammatory status in adipocytes. Although the molecular mechanism of complex formation remains elusive, we suspect that it is similar to the interaction of protein Sirt3/IDH2 by directly deacetylation, and this needs further study.[42,61] From these findings, we surmise that melatonin participates in the regulation of inflammatory responses by αKG-mediated epigenetic reprogramming in adipose tissue.

Exosomes have been considered as important mediators of cell-cell communication by exchange of material and delivering information.[29] Studies have determined that adipocytes can release exosomes to recipient cells and tissues thereby modifying the physiological state of the recipient cells.[62,63] Here, we demonstrated that melatonin increased exosomes secretion from adipocytes and elevated the αKG concentration in

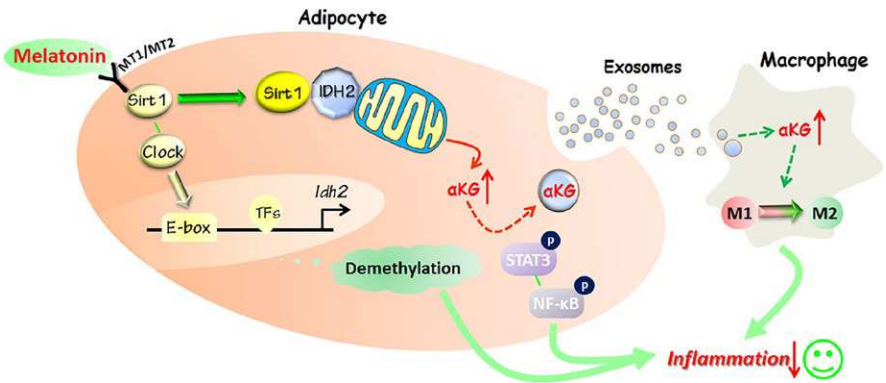


**FIGURE 10** Melatonin coordinates inflammatory response through elevating αKG and diverting to macrophages via exosomes in mice adipose tissue. Melatonin alleviated inflammatory response through increasing cellular and exosomal αKG level in adipose tissue. Exosomal αKG transports to recipient macrophages and performs the anti-inflammatory function by epigenetic reprogramming

adipose-derived exosomes. Notably, we are the first demonstrated that exosomes (secretion from melatonin-treated adipocytes) subsequently transported to macrophages and acted as a critical switch governing M1 and M2 macrophage polarization. In addition, further analysis suggested that αKG inhibited inflammation response in macrophage through epigenetic reprogramming. These findings are consistent with other studies that αKG regulated the immune responses of macrophages through metabolic and epigenetic reprogramming.[57,64] Our previous study had determined that melatonin inhibited inflammasome formation and pyroptosis in adipocytes.[27] We then assumed that exosomal αKG was essential for the inhibitory role of melatonin on inflammation of neighboring adipocytes. In our study, we showed that exosomal αKG decreased adipocyte inflammation along with the reduction of phosphorylation of STAT3/NF-κB signal. Notably, we are the first to point out a significant correlation between circadian clock and αKG concentration. The regulatory mechanism of *Clock* on gene transcription may depend on E-box, which is a DNA response element.[65] We hypothesized that melatonin elevated cellular and exosomal αKG level associated with the binding of *Clock* to E-box in the promoter region of *Idh2* during adipocyte inflammation. Although we and other studies have determined melatonin and αKG coordinately alleviated inflammation, the precise mechanisms that melatonin regulates exosomal αKG secretion need to be further studied.[66,67]

There are also several limitations in this study. First, the dose of melatonin we used was at a pharmacological level. However, we and others suggested that this dose did not affect the viability of adipocytes[26,27] and could affect many biological processes in adipocytes.[68-70] Second, we did not confirm whether melatonin affects other metabolites in exosomes that may play important functional roles during adipose inflammation. In addition, it is possible that multiple metabolites within the exosomes could work in a coordinated way to reduce adipose inflammation that we have observed. Future metabolomics study will be necessary to demonstrate the full set of melatonin regulating the adipose-derived exosomes.

In summary, our present study demonstrates that melatonin alleviates inflammatory response through increasing cellular and exosomal αKG level in adipose tissue. Moreover, adipose-derived exosomes transport to recipient macrophages and perform the anti-inflammatory function by αKG-regulated epigenetic reprogramming (Figure 10). Thus, our results indicate that melatonin can be potentially used in the therapy of obesity-associated metabolic disease by delivering desirable information to an accurate target cell.

## ACKNOWLEDGEMENTS

This work was supported by the grants from the Major National Scientific Research Projects (2015CB943102) and the National Nature Science Foundation of China (31572365) and Key Sci-tech innovation team of Shaanxi province (2017KCT-24) and the Fundamental Research Funds for the Central Universities (2452017084). We appreciated Prof. Shimin Liu from School of Animal Biology, The University of Western Australia to help us improve the English writing.

## AUTHOR CONTRIBUTIONS

All the authors were contributed to this manuscript. Z.L., L.G., and C.S. planned the experiments. All the authors performed the experiments. L.G., T. Z., and Q.R. analyzed the data. Z.L., Q.R., and T.Z. contributed reagents or other essential material. Z.L. and L.G. wrote the manuscript.

## CONFLICT OF INTEREST

The authors declare that there is no duality of interest associated with this manuscript.

## ORCID

*Chao Sun* http://orcid.org/0000-0001-7222-4028

## REFERENCES

1. Szewczyk-golec K, Wozniak A, Reiter RJ. Inter-relationships of the chronobiotic, melatonin, with leptin and adiponectin: implications for obesity. *J Pineal Res*. 2015;59:277-291.
2. Reilly SM, Saltiel AR. Adapting to obesity with adipose tissue inflammation. *Nat Rev Endocrinol*. 2017;13:633-643.
3. Lumeng CN, Saltiel AR. Inflammatory links between obesity and metabolic disease. *J Clin Invest*. 2011;121:2111-2117.
4. Shan B, Wang X, Wu Y, et al. The metabolic ER stress sensor IRE1alpha suppresses alternative activation of macrophages and impairs energy expenditure in obesity. *Nat Immunol*. 2017;18:519-529.
5. Brestoff JR, Artis D. Immune regulation of metabolic homeostasis in health and disease. *Cell*. 2015;161:146-160.
6. Mcnelis Joanne C, Olefsky-jerrold M. Macrophages, immunity, and metabolic disease. *Immunity*. 2014;41:36-48.
7. Lampropoulou V, Sergushichev A, Bambouskova M, et al. Itaconate links inhibition of succinate dehydrogenase with macrophage metabolic remodeling and regulation of inflammation. *Cell Metab*. 2016;24:158-166.
8. Mills E, O'neill LA. Succinate: a metabolic signal in inflammation. *Trends Cell Biol*. 2014;24:313-320.
9. Hardeland R, Madrid JA, Tan DX, et al. Melatonin, the circadian multioscillator system and health: the need for detailed analyses of peripheral melatonin signaling. *J Pineal Res*. 2012;52:139-166.
10. Agil A, El-hammadi M, Jimenez-aranda A, et al. Melatonin reduces hepatic mitochondrial dysfunction in diabetic obese rats. *J Pineal Res*. 2015;59:70-79.
11. Alonso-vale MI, Andreotti S, Mukai PY, et al. Melatonin and the circadian entrainment of metabolic and hormonal activities in primary isolated adipocytes. *J Pineal Res*. 2008;45:422-429.

12. Manchester LC, Coto-montes A, Boga JA, et al. Melatonin: an ancient molecule that makes oxygen metabolically tolerable. *J Pineal Res*. 2015;59:403-419.
13. Mauriz JL, Collado PS, Veneroso C, et al. A review of the molecular aspects of melatonin's anti-inflammatory actions: recent insights and new perspectives. *J Pineal Res*. 2013;54:1-14.
14. Reiter RJ. Pineal melatonin: cell biology of its synthesis and of its physiological interactions. *Endocr Rev*. 1991;12:151-180.
15. Alvarez-sanchez N, Cruz-chamorro I, Diaz-sanchez M, et al. Melatonin reduces inflammatory response in peripheral T helper lymphocytes from relapsing-remitting multiple sclerosis patients. *J Pineal Res*. 2017;63:e12442.
16. Slominski RM, Reiter RJ, Schlabritz-loutsevitch N, et al. Melatonin membrane receptors in peripheral tissues: distribution and functions. *Mol Cell Endocrinol*. 2012;351:152-166.
17. Zhao L, An R, Yang Y, et al. Melatonin alleviates brain injury in mice subjected to cecal ligation and puncture via attenuating inflammation, apoptosis, and oxidative stress: the role of SIRT1 signaling. *J Pineal Res*. 2015;59:230-239.
18. Cano Barquilla P, Pagano ES, Jimenez-ortega V, et al. Melatonin normalizes clinical and biochemical parameters of mild inflammation in diet-induced metabolic syndrome in rats. *J Pineal Res*. 2014;57:280-290.
19. Chen J, Qian C, Duan H, et al. Melatonin attenuates neurogenic pulmonary edema via the regulation of inflammation and apoptosis after subarachnoid hemorrhage in rats. *J Pineal Res*. 2015;59:469-477.
20. Brazao V, Santello FH, Colato RP, et al. Melatonin: antioxidant and modulatory properties in age-related changes during trypanosoma cruzi infection. *J Pineal Res*. 2017;63:12409.
21. Muxel SM, Laranjeira-silva MF, Carvalho-sousa CE, et al. The RelA/cRel nuclear factor-kappaB (NF-kappaB) dimer, crucial for inflammation resolution, mediates the transcription of the key enzyme in melatonin synthesis in RAW 264.7 macrophages. *J Pineal Res*. 2016;60:394-404.
22. MEdrano-campillo P, Sarmiento-soto H, Alvarez-sanchez N, et al. Evaluation of the immunomodulatory effect of melatonin on the T-cell response in peripheral blood from systemic lupus erythematosus patients. *J Pineal Res*. 2015;58:219-226.
23. Radogna F, Paternoster L, Albertini MC, et al. Melatonin antagonizes apoptosis via receptor interaction in U937 monocytic cells. *J Pineal Res*. 2007;43:154-162.
24. Calvo JR, Gonzalez-yanes C, Maldonado MD. The role of melatonin in the cells of the innate immunity: a review. *J Pineal Res*. 2013;55:103-120.
25. Xia MZ, Liang YL, Wang H, et al. Melatonin modulates TLR4-mediated inflammatory genes through MyD88- and TRIF-dependent signaling pathways in lipopolysaccharide-stimulated RAW264.7 cells. *J Pineal Res*. 2012;53:325-334.
26. Liu Z, Gan L, Luo D, et al. Melatonin promotes circadian rhythm-induced proliferation through Clock/histone deacetylase 3/c-Myc interaction in mouse adipose tissue. *J Pineal Res*. 2017;62:e12383.
27. Liu Z, Gan L, Xu Y, et al. Melatonin alleviates inflammasome-induced pyroptosis through inhibiting NF-kappaB/GSDMD signal in mice adipose tissue. *J Pineal Res*. 2017;63:e12414.
28. EL Andaloussi S, Mager I, Breakefield XO, et al. Extracellular vesicles: biology and emerging therapeutic opportunities. *Nat Rev Drug Discov*. 2013;12:347-357.
29. Tkach M, Thery C. Communication by extracellular vesicles: where we are and where we need to go. *Cell*. 2016;164:1226-1232.
30. Fan R, Toubal A, Goni S, et al. Loss of the co-repressor GPS2 sensitizes macrophage activation upon metabolic stress induced by obesity and type 2 diabetes. *Nat Med*. 2016;22:780-791.
31. Lackey DE, Olefsky JM. Regulation of metabolism by the innate immune system. *Nat Rev Endocrinol*. 2016;12:15-28.
32. Laranjeira-silva MF, Zampieri RA, Muxel SM, et al. Melatonin attenuates *Leishmania* (L.) amazonensis infection by modulating arginine metabolism. *J Pineal Res*. 2015;59:478-487.
33. Shi H, Chen Y, Tan DX, et al. Melatonin induces nitric oxide and the potential mechanisms relate to innate immunity against bacterial pathogen infection in *Arabidopsis*. *J Pineal Res*. 2015;59:102-108.
34. Youm YH, Nguyen KY, Grant RW, et al. The ketone metabolite beta-hydroxybutyrate blocks NLRP3 inflammasome-mediated inflammatory disease. *Nat Med*. 2015;21:263-269.
35. Husted AS, Trauelsen M, Rudenko O, et al. GPCR-mediated signaling of metabolites. *Cell Metab*. 2017;25:777-796.
36. Carey BW, Finley LW, Cross JR, et al. Intracellular alpha-ketoglutarate maintains the pluripotency of embryonic stem cells. *Nature*. 2015;518:413-416.
37. Eming SA, Wynn TA, Martin P. Inflammation and metabolism in tissue repair and regeneration. *Science*. 2017;356:1026-1030.
38. Kettner NM, Mayo SA, Hua J, et al. Circadian dysfunction induces leptin resistance in mice. *Cell Metab*. 2015;22:448-459.
39. Gan L, Liu Z, Feng F, et al. Foxc2 coordinates inflammation and browning of white adipose by leptin-STAT3-PRDM16 signal in mice. *Int J Obes*. 2017;208: in press.
40. Yang H, Hreggvidsdottir HS, Palmblad K, et al. A critical cysteine is required for HMGB1 binding to Toll-like receptor 4 and activation of macrophage cytokine release. *Proc Natl Acad Sci USA*. 2010;107:11942-11947.
41. Li W, Li J, Ashok M, et al. A cardiovascular drug rescues mice from lethal sepsis by selectively attenuating a late-acting proinflammatory mediator, high mobility group box 1. *J Immunol*. 2007;178:3856-3864.
42. Someya S, Yu W, Hallows WC, et al. Sirt3 mediates reduction of oxidative damage and prevention of age-related hearing loss under caloric restriction. *Cell*. 2010;143:802-812.
43. Deng ZB, Poliakov A, Hardy RW, et al. Adipose tissue exosome-like vesicles mediate activation of macrophage-induced insulin resistance. *Diabetes*. 2009;58:2498-2505.
44. Campoy I, Lanau L, Altadill T, et al. Exosome-like vesicles in uterine aspirates: a comparison of ultracentrifugation-based isolation protocols. *J Transl Med*. 2016;14:180.
45. Mincheva-nilsson L, Baranov V, Nagaeva O, et al. Isolation and characterization of exosomes from cultures of tissue explants and cell lines. *Curr Protoc Immunol*. 2016;115:14421-14422.
46. Reik W. Stability and flexibility of epigenetic gene regulation in mammalian development. *Nature*. 2007;447:425-432.
47. Tahiliani M, Koh KP, Shen Y, et al. Conversion of 5-methylcytosine to 5-hydroxymethylcytosine in mammalian DNA by MLL partner TET1. *Science*. 2009;324:930-935.
48. Yang Q, Liang X, Sun X, et al. AMPK/alpha-ketoglutarate axis dynamically mediates DNA demethylation in the Prdm16 promoter and brown adipogenesis. *Cell Metab*. 2016;24:542-554.

49. Yang Y, Jiang S, Dong Y, et al. Melatonin prevents cell death and mitochondrial dysfunction via a SIRT1-dependent mechanism during ischemic-stroke in mice. *J Pineal Res*. 2015;58:61-70.
50. Crooke A, Huete-toral F, Colligris B, et al. The role and therapeutic potential of melatonin in age-related ocular diseases. *J Pineal Res*. 2017;63:e12430.
51. Hardeland R. Melatonin and the theories of aging: a critical appraisal of melatonin's role in antiaging mechanisms. *J Pineal Res*. 2013;55:325-356.
52. Agil A, Reiter RJ, Jimenez-aranda A, et al. Melatonin ameliorates low-grade inflammation and oxidative stress in young zucker diabetic fatty rats. *J Pineal Res*. 2013;54:381-388.
53. Carlberg C, Wiesenberg I. The orphan receptor family RZR/ROR, melatonin and 5-lipoxygenase: an unexpected relationship. *J Pineal Res*. 1995;18:171-178.
54. Cervenka I, Agudelo LZ, Ruas JL. Kynurenines: tryptophan's metabolites in exercise, inflammation, and mental health. *Science*. 2017;357:eaaf9794.
55. Ungaro F, Tacconi C, Massimino L, et al. MFSD2A promotes endothelial generation of inflammation-resolving lipid mediators and reduces colitis in mice. *Gastroenterology*. 2017;153:1363-1377.
56. Prochnicki T, Latz E. Inflammasomes on the crossroads of innate immune recognition and metabolic control. *Cell Metab*. 2017;26:71-93.
57. Liu PS, Wang H, Li X, et al. alpha-ketoglutarate orchestrates macrophage activation through metabolic and epigenetic reprogramming. *Nat Immunol*. 2017;18:985-994.
58. Zavodnik IB, Lapshina EA, Cheshchevik VT, et al. Melatonin and succinate reduce rat liver mitochondrial dysfunction in diabetes. *J Physiol Pharmacol*. 2011;62:421-427.
59. Das N, Mandala A, Naaz S, et al. Melatonin protects against lipid-induced mitochondrial dysfunction in hepatocytes and inhibits stellate cell activation during hepatic fibrosis in mice. *J Pineal Res*. 2017;62:e12404.
60. Wu H, Zhang Y. Reversing DNA methylation: mechanisms, genomics, and biological functions. *Cell*. 2014;156:45-68.
61. Zou X, Zhu Y, Park SH, et al. SIRT3-mediated dimerization of IDH2 directs cancer cell metab. and Tumor Growth. *Cancer Res*. 2017;77:3990-3999.
62. Thomou T, Mori MA, Dreyfuss JM, et al. Adipose-derived circulating miRNAs regulate gene expression in other tissues. *Nature*. 2017;542:450-455.
63. Holmes D. Adipose tissue: adipocyte exosomes drive melanoma progression. *Nat Rev Endocrinol*. 2016;12:436.
64. Hwang IY, Kwak S, Lee S, et al. Psat1-dependent fluctuations in alpha-ketoglutarate affect the timing of ESC differentiation. *Cell Metab*. 2016;24:494-501.
65. Vriend J, Reiter RJ. Melatonin feedback on clock genes: a theory involving the proteasome. *J Pineal Res*. 2015;58:1-11.
66. Li Z, Nickkholgh A, Yi X, et al. Melatonin protects kidney grafts from ischemia/reperfusion injury through inhibition of NF-kB and apoptosis after experimental kidney transplantation. *J Pineal Res*. 2009;46:365-372.
67. Kruidenier L, Chung CW, Cheng Z, et al. A selective jumonji H3K27 demethylase inhibitor modulates the proinflammatory macrophage response. *Nature*. 2012;488:404-408.
68. Kato H, Tanaka G, Masuda S, et al. Melatonin promotes adipogenesis and mitochondrial biogenesis in 3T3-L1 preadipocytes. *J Pineal Res*. 2015;59:267-275.
69. Alonso-vale MI, Peres SB, Vernochet C, et al. Adipocyte differentiation is inhibited by melatonin through the regulation of C/EBPbeta transcriptional activity. *J Pineal Res*. 2009;47:221-227.
70. Wu SM, Lin WY, Shen CC, et al. Melatonin set out to ER stress signaling thwarts epithelial mesenchymal transition and peritoneal dissemination via calpain-mediated C/EBPbeta and NFkappaB cleavage. *J Pineal Res*. 2016;60:142-154.


**How to cite this article:** Liu Z, Gan L, Zhang T, Ren Q, Sun C. Melatonin alleviates adipose inflammation through elevating α-ketoglutarate and diverting adipose-derived exosomes to macrophages in mice. *J Pineal Res*. 2018;64:e12455. https://doi.org/10.1111/jpi.12455